Macromolecules
ARTICLE

Macromolecules **2009**, *42*, 4319–4327 **4319**
DOI: 10.1021/ma9004007

Molecular Simulation of Cross-Linked Epoxy and Epoxy−POSS Nanocomposite

Po-Han Lin and Rajesh Khare*

Department of Chemical Engineering, Texas Tech University, Box 43121, Lubbock, Texas 79409-3121

Received February 20, 2009; Revised Manuscript Received April 21, 2009

ABSTRACT: We present an efficient method for the creation of atomistic model structures of cross-linked polymer matrices. The method consists of preparation of a physical mixture of the monomer and the cross-linker molecules in the box followed by a single-step polymerization of the entire mixture. For this purpose, the simulated annealing algorithm is used to identify pairs of reacting atoms that are spatially close. The technique is used to create five structures of cross-linked epoxy as well as cross-linked epoxy−POSS (i.e., polyhedral oligomeric silsesquioxane) nanocomposite. The models so generated are characterized with respect to the density, volume−temperature behavior, and the detailed molecular structure. Our results show that incorporation of POSS particles (at 5 wt %) in the cross-linked epoxy resin leads to a weak tendency for lowering the coefficient of volume thermal expansion but does not cause a measurable change in the glass transition temperature.

Introduction

Thermosetting epoxy is widely used in applications in the areas of aerospace and electronics due to its superior mechanical properties.[1] However, the development of residual thermal stresses during the curing process poses problems in these applications, and thus minimization of this effect by, for example, incorporation of nanofillers in the epoxy matrix remains an active area of research. The nanocomposites formed by the incorporation of inorganic nanofillers (e.g., clay, polyhedral oligomeric silsesquioxane, i.e., POSS) in polymeric matrices have the potential for the creation of high-performance materials resulting from the combination of the properties of their components.[2,3] Theoretical and simulation approaches can be used to describe the complex physical and chemical interactions in these systems in order to predict their properties.[4] POSS nanoparticles have cage-type structures with a silica-like core to which organic functional groups can be attached. Properties of POSS particles can be tailored by chemical substitution of the functional groups on these side chains that are attached to the central cage. In this work, we employ the technique of molecular simulation to study both cross-linked epoxy and a nanocomposite formed by the incorporation of the POSS nanoparticles into a cross-linked epoxy matrix via chemical bonding. For over two decades, molecular simulations have been employed for predicting the properties of amorphous polymers. Such a simulation approach consists of generating atomistically detailed model structures of the polymers of interest and then using statistical mechanics to determine the thermomechanical properties of these materials. The specific chemical interactions in the system are accounted by the force field parameters that have been developed and fine-tuned over the years.

For linear polymers and polymers with short branches, the model structures of dense amorphous systems are generated either by constructing the chains in a bond-by-bond fashion in the simulation box[5] or by "melting" an ordered array of chains (crystal of the polymer, if the crystal structure is known).[6] The former method encounters difficulties when the monomer unit to be added in the chain growth process is large (several intermediate stages are required in that case)[7,8] or for chains with a complex architecture. The latter method requires that the crystal structure of the polymer be known or at least that one should be able to create a reasonable, ordered arrangement of chains which will serve as the starting point for the "melting" process. For polymers with large monomer units, alternate approaches such as polymerization of the monomer mixture in the simulation box[9,10] or first creating a coarse-grained model structure and then converting it to an atomistic model have been proposed.[11,12] Cross-linked epoxy structure is characterized by both—a large monomer unit (which is the case for commonly used epoxy materials) and a complex topology—thus necessitating special considerations for building atomistic model structures of these systems.

Approaches that have been used in the literature for building structures of cross-linked matrices can be broadly classified into two categories: (1) building a cross-linked network structure using a coarse-grained model and then converting the coarse-grained model back to the atomistic description[13] and (2) starting with a physical mixture of monomer and cross-linker molecules and then "polymerizing" the mixture in conjunction with molecular dynamics (MD) simulation. The first approach has previously been used for building model structures of amorphous polystyrene and cellulose.[11,12] Recently, Komarov et al. built a structure of cross-linked epoxy using a four-step version of this method that involved creating a cross-linked network using a coarse-grained model, relaxing this structure using Monte Carlo simulation, reverse mapping back to atomistic representation, and then relaxing the atomistic model structure using MD simulation.[13]

The second approach—polymerization of a physical mixture of the atomistically modeled monomers—has been applied for generating structures of polyethylene,[9] polystyrene,[10] polymethacrylate networks,[14] poly(dimethylsiloxane) networks,[15] and cross-linked epoxy.[16−18] In this procedure, the polymerization can be implemented in either a single step[9,10,16] (where all of the potential chemical bonds between monomers are formed at the beginning) or in many steps[14,15,17,18] (where the system is relaxed using molecular mechanics or MD simulation and the reacting atom pairs that approach within a specified cutoff distance are bonded).

In the multistep process, the local strain generated in the system due to the creation of the new bonds is relieved by relaxing

*To whom correspondence should be addressed.

Published on Web 05/21/2009

the system using MD simulation in each step. This approach is thus expected to lead to the creation of a well-relaxed structure. The multistep process can be implemented by creating only one new bond per step or iteration. A modification consists of creating multiple bonds (between all pairs of reactive sites that are within a chosen cutoff distance) per step; when such a "dynamic cross-linking approach" was applied to an epoxy system that could form 256 cross-links, most of the new bonds were created in 75 iterations.[18] The single-step process offers the possibility for faster generation of the structures but could potentially be hampered by the large strain created in the system due to simultaneous formation of the chemical bonds, many of which will be between atoms that reside at distances much larger than the bond length. In this work, we have addressed this problem by extending the simulated annealing polymerization approach that was previously used by one of us for generating structures of polystyrene.[10] It is shown that the approach can be used for single-step polymerization for generating structures of cross-linked epoxy as well as a nanocomposite formed by chemical incorporation of POSS molecules in an epoxy system.

The rest of the paper is organized as follows. We begin with a description of the molecular models that are used in this work. This is followed by a detailed description of the algorithm used for generating the structure of the cross-linked epoxy as well as the cross-linked epoxy−POSS nanocomposite. The structures so built are characterized with respect to the properties such as the volume−temperature ($V-T$) behavior, glass transition temperature, and molecular scale packing. We close with a discussion of our structure building procedure and a summary of the results.

Simulation Method

A. Molecular Models, Force Field, and Simulation Details. The system studied consisted of diglycidyl ether bisphenol A (DGEBA) as the epoxy monomer and trimethylene glycol di-*p*-aminobenzoate (TMAB) as the cross-linker; the particular POSS molecule studied is octaglycidoxypropyl POSS. The chemical structures of these molecules are shown in Figure 1. The curing reaction consists of the reaction of the hydrogen atoms in the amine group with the epoxide group (see Figure 2). In this work, the molecular models were built using the XLEaP program in the AMBER package.[19] The molecular topology was created using the antechamber[20] program in AmberTools 1.2, and the partial charges on the atoms were assigned using the AM1-BCC method.[21,22] For some atoms, large discrepancies were observed between the values so calculated and the partial charge values in the literature.[23−25] The partial charge values were adjusted to alleviate these discrepancies and were also symmetrized to account for the symmetry of the epoxy and cross-linker molecules. Both molecules were described by the general AMBER force field (gaff)[26,27] supplemented by literature parameter values.[25,28,29] The values of the additional parameters as well as the final values of these partial charges are given in the Supporting Information.

The molecular dynamics simulations and the energy minimizations were carried out using the GROMACS 3.3.3 package.[30−32] For MD simulations, a time step of 1 fs was used. A cutoff distance of 10 Å (with the buffer of 1 Å) was used for the van der Waals interactions, whereas the particle mesh Ewald (PME) algorithm[33] was used to handle the electrostatic interactions. The temperature and pressure values were controlled using the Nose−Hoover thermostat[34,35] and the Parrinello−Rahman[36,37] methods, respectively.

B. Structure Building Procedure. The structures of cross-linked epoxy and cross-linked epoxy−POSS nanocomposite were generated in this work by polymerizing the mixture of

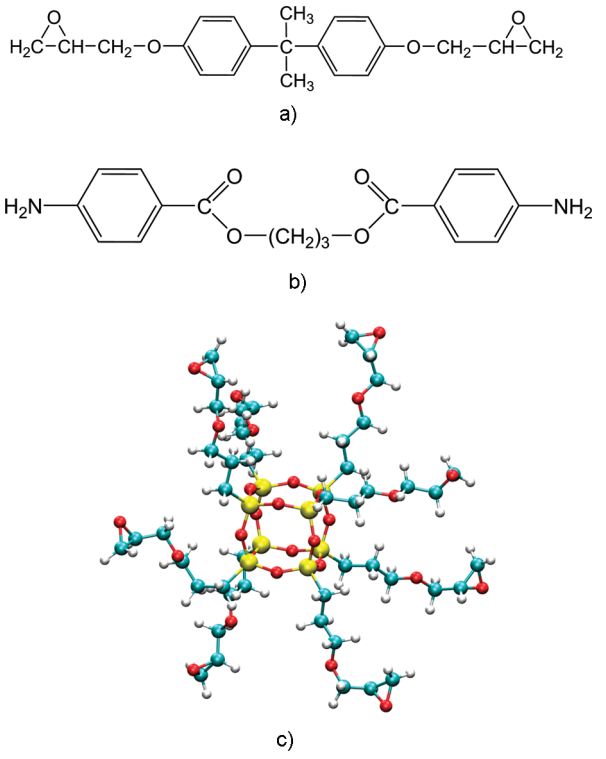

Figure 1. Chemical structures of the (a) DGEBA (epoxy monomer), (b) TMAB (cross-linker), and (c) the POSS molecule. For the POSS molecule, carbon, oxygen, silicon, and hydrogen atoms are shown in blue, red, yellow, and white color, respectively.

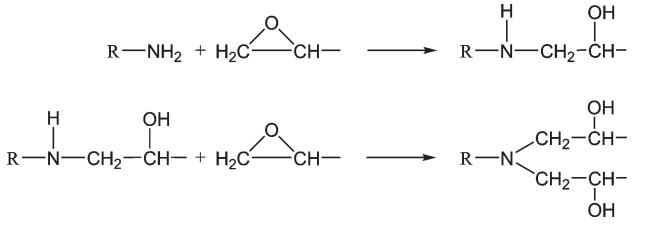

Figure 2. Schematic of the cross-linking reaction.

the epoxy monomers and the cross-linkers in the simulation box. In order to form an initial structure that is free of large strain, the bond lengths for the newly created bonds in the polymerization step must be comparable to the equilibrium bond lengths. A random choice of bonding pairs breaks this requirement, and hence in general, one needs to identify pairs of bonding atoms on the epoxy monomer and cross-linker molecules that are spatially close to each other. Identification of the set of such spatially close pairs of bonding atoms thus becomes the most challenging task in this process. Mathematically, this is a multivariable optimization problem where collectively for all of the newly created bonds a chosen cost function based on the bond lengths must be at a minimum. In previous work involving the polymerization of styrene monomers, such a problem was solved using the simulated annealing optimization technique.[38] In that work,[10] after preparing a physical mixture of styrene monomers in the simulation box, the shortest path connecting these monomers was obtained using the simulated annealing optimization technique. Polystyrene model structures were then created by forming bonds between the spatially close monomers so identified and relaxing the structures using a combination of energy minimization and molecular dynamics simulation. In this work, we have extended this approach to incorporate the modifications required to

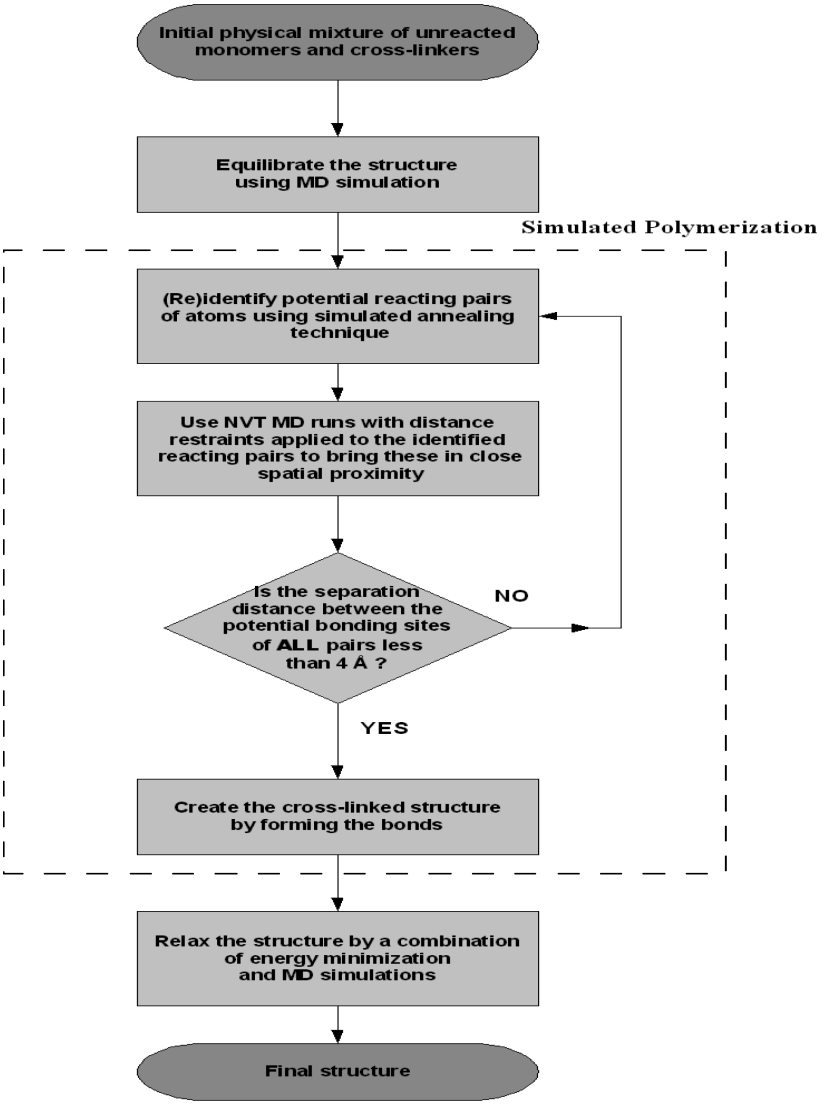

Figure 3. Outline of the simulated annealing polymerization procedure.

account for the complexities (e.g., the number of connections) of the unreacted epoxy monomer, cross-linker, and POSS molecules. A succinct overview of the procedure is facilitated by presentation in form of a flowchart;[18] such a flowchart for our proposed approach is shown in Figure 3, and the specific details are given in what follows.

The first step in the process consists of generating a "reaction mixture" containing the stoichiometric amounts of the monomer and the cross-linker molecules. For the neat epoxy system, we prepared an initial mixture consisting of 100 monomer and 50 cross-linker molecules placed in a cubic box at a low density of 0.1 g/cm^3. This system was then compressed to a density close to 1.0 g/cm^3 using a short constant *NPT* (constant number of molecules, constant pressure, and constant temperature) MD run at 500 atm and 300 K. A randomly arranged mixture of these unreacted molecules was then obtained by further carrying out a 200 ps long constant *NVT* (constant number of molecules, constant volume, and constant temperature) MD run at 600 K. This reaction mixture was scanned for determining the spatially close pairs of bonding atoms on the monomers and cross-linkers that can potentially form bonds in the polymerization step. This problem is mathematically analogous to the traveling salesman problem and is solved here using the simulated annealing technique.

The simulated annealing algorithm initially picks a random path (i.e., sequence of bonds between randomly picked reacting site pairs) that connects all of the potential reacting sites in the simulation box. The simulated annealing technique implementation is similar to the constant *NVT* Monte Carlo (MC) simulation in statistical mechanics where the sum of the bond lengths in our system is analogous to the energy in MC and a chosen length scale is analogous to the factor kT, where k is the Boltzmann constant and T is the temperature. In a manner similar to MC simulation, the algorithm proceeds by proposing a "move" to alter the initial bonding sequence. In this work, only one type of move—path reversal—is employed for this purpose.[39] This move consists of first selecting a segment of a randomly chosen length and which is at a randomly chosen location along the chain. The bonding sequence of the molecules along this path is then reversed. We note that as a result of this move only the bonds at the two end points of the selected path segment get altered. This proposed change in the bonding sequence (analogous to MC move) is either accepted or rejected using a criterion (which is analogous to the move acceptance probability in MC simulation) that utilizes the change in the bond lengths resulting from the proposed move. The initial value of the length scale (analogous to the factor kT in MC simulation) is chosen to be

2.5 Å in this work. The system is annealed by reducing the length scale value by a factor of 0.95 when either one of the following conditions gets satisfied:

$$\text{(no. of attempted moves)} = 100 \times \text{(no. of reactive pairs in the box)}$$

or

$$\text{(no. of accepted moves)} = 10 \times \text{(no. of reactive pairs in the box)}$$

Consecutive application of these path alteration moves in conjunction with the above annealing schedule leads to a bond connectivity path that minimizes the sum of lengths of the bonds formed by joining the unreacted monomer and the cross-linker molecules. In practice, this simulated annealing step takes less than 15 min of CPU time for our model systems.

The bonding sequence suggested by simulated annealing is assessed for viability of creating bonds that will result in a well-relaxed cross-linked structure. For this purpose, ideally, the distance between these potential bonding sites should be close to the C−N bond length, i.e., 1.364 Å. However, in the unbonded state, the closest distance of approach between these atoms is governed by the van der Waals diameter of these atoms (~3.4 Å). In practice, most potentially reacting pairs in the initial configuration reside at even greater distances which, if connected, lead to severe problems during the process of relaxation of the generated cross-linked structures. This issue was addressed by using the following procedure. These structures were subjected to two NVT MD runs of 50 ps duration at 300 K; harmonic distance restraints (8 Å for the first run and 3 Å for the second run) were applied to the identified reactive pairs during these MD runs in order to bring these in close spatial proximity. We note that such a step was not required in the application of simulated polymerization approach to polystyrene[10] but is required here for the cross-linked epoxy systems. Following these MD runs, the structures were again scanned to check if the separation distance between all of the reacting atom pairs is less than 4 Å. If this were not to be the case, the structure would be subjected to another simulated annealing sequencing step (see the possible iteration loop in Figure 3). In practice, such iteration was not required for any of the cross-linked epoxy structures that were generated in this work. In the final step, chemical bonds were created between the identified reacting sites. The final structure thus obtained was relaxed by energy minimization using the conjugate gradients method which usually converged within 200 steps, although up to 600 steps were required in some cases. The structures were further relaxed by subjecting these to NPT MD simulation at 600 K for 3 ns, followed by stepwise cooling down to 300 K at a rate of 15 K/200 ps.

The same approach was used for building structures of cross-linked epoxy−POSS nanocomposite. In this case, the simulated system consisted of 200 epoxy monomer, 108 cross-linker, and 4 POSS molecules; this corresponds to 5 wt % POSS in the system while maintaining the stoichiometric ratio of epoxide groups and amino hydrogen atoms in the system. The epoxide groups on both the epoxy monomers and the 8 arms of the POSS cage participate in the cross-linking reaction with the amine groups on TMAB cross-linker molecules. An additional consideration needs to be accounted for in this case—a cross-linker molecule can form bonds with the epoxide groups on the two arms of the same POSS cage, thus leading to the formation of "intramolecular" or short loops in the system. In order to judge the possibility of occurrence of such "intramolecular" loops, we calculated the radial distribution function (RDF) for the end carbon atoms of the epoxide groups on the arms of the same POSS cage and the RDF for the nitrogen atoms of the amine groups of the same cross-linker molecule in the unreacted state at 433 K (Figure 4), which is in the range of temperatures where the curing reaction is typically carried out. As can be seen, the carbon atoms of the epoxide groups on the same POSS cage predominantly reside in a separation range of 0.3−2.0 nm, whereas the distribution of the separation distance between the N atoms of the two amine groups of the cross-linker is bimodal with peaks around 0.5 and 1.5 nm. The significant overlap between the distances spanned by these two distributions indicates a possibility for the formation of at least a few of these intramolecular loops during the cross-linking reaction. A systematic study of such intramolecular cross-links and their effect on the properties (if any) is a separate topic of study in itself; in this work, our algorithm explicitly precludes the formation of such intramolecular cross-links. With this exception, the rest of the simulated annealing and structure building procedure is the same for the epoxy−POSS structures as for the neat cross-linked epoxy structures. The only other difference we note is that while no iterations (see Figure 3 and earlier text) in the structure generation process were required for cross-linked epoxy, up to three iterations were required in the building process for epoxy−POSS nanocomposite structures that we built. The simulated annealing step itself required 30 min of CPU time for the cross-linked epoxy−POSS system. Figure 5 shows a snapshot of an atomistic model structure of an epoxy−POSS nanocomposite that was built using the above procedure.

C. Structure Relaxation and Determination of Volume−Temperature Behavior. The cross-linked epoxy and cross-linked epoxy−POSS structures prepared using the above method are at a temperature of 300 K, which is below the glass transition temperature of these materials. In order to obtain well-relaxed structures, we used MD simulation to heat these to a temperature of 600 K, which is well above the glass transition temperature. These structures at 600 K were then cooled in a stepwise fashion to 300 K. For this, the temperature was lowered in steps of 15 K and at each temperature; the system was relaxed by constant NPT MD simulation for 2 ns duration. An inspection of the density of the system during these MD runs indicated that at each temperature the system density reached a new average value (started fluctuating about a new average value) within the first 500 ps of MD simulation. In addition to obtaining the well-relaxed structures at 300 K, such a procedure also yields information on the volume−temperature ($V-T$) behavior of these systems. Both the glass transition temperature and the coefficient of thermal expansion (for both glassy and rubbery states) are also evaluated from these $V-T$ data.

Results

The simulated polymerization approach was used to generate five structures for cross-linked epoxy as well as POSS−epoxy nanocomposite. These structures were characterized with respect to volumetric and structural properties.

A. Volumetric Properties. Figure 6 shows the temperature dependence of the specific volume of the cross-linked epoxy structure. As described earlier, the structures were subjected to MD simulation at each temperature for 2 ns; the specific volume was determined from the second half of this duration. The uncertainties were determined from simulations on the five structures that were generated and are also shown in the figure. As can be seen from the figure, the

specific volume shows a linear relationship with temperature at temperatures both higher (rubbery region) and lower (glassy region) than the glass transition temperature. The glass transition temperature (T_g) can be determined from the point of intersection of the linear fits to these $V-T$ data in the rubbery and glassy regions. Given the uncertainties in the simulated values of specific volume, we determined the uncertainty in the T_g by creating a large number of data sets in which specific volume at each temperature was sampled from a range around the mean value bound by the uncertainty[39] and then determining the point of intersection of the linear fits in the glassy and rubbery regions. The T_g obtained using this procedure for cross-linked epoxy is 480 ± 17 K. This value is about 27 K higher than the experimental value of 453 K for the same system.[40−42] When making this comparison, we also note that although the experimentally measured glass transition temperature is oftentimes the T_f', i.e., the limiting fictive temperature determined from DSC;[41] this T_f' is expected to be a very close approximation to the T_g.[43] The larger value of T_g in simulations is to be expected given that the cooling rates employed in the simulation are orders of magnitude higher than those used in a typical experimental determination of T_g. In addition, the density of the cross-linked epoxy at 300 K is 1.187 ± 0.008 g/cm^3. Experimentally, the density of this cross-linked epoxy system has been reported to be either in the range of 1.21−1.225[40,42,44,45] or 1.35 g/cm^3.[41] The density of cross-linked epoxy predicted from simulation is within 3% of the former value. The lower value of the density observed in the simulations is consistent with the higher glass transition temperature that is observed in the simulations since early formation of glass upon cooling is expected to yield a glass with a lower density.

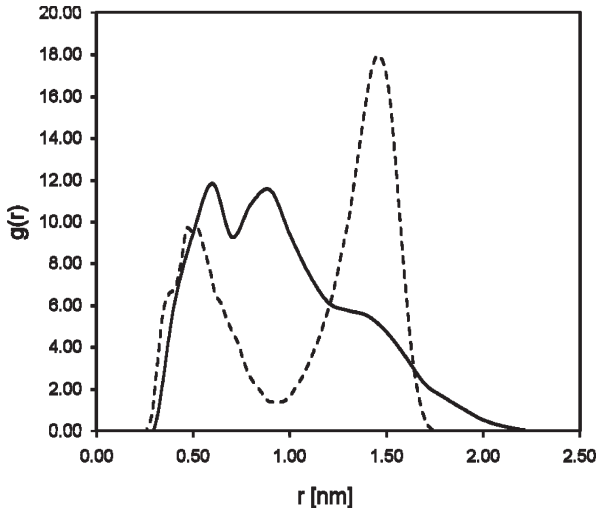

Figure 4. Radial distribution functions for end carbon atoms of the arms of the POSS (solid line) and end nitrogen atoms of the cross-linker molecules (dashed line).

The dependence of specific volume on the temperature for the cross-linked epoxy−POSS structures is shown in Figure 7. Once again, the data show a linear dependence of

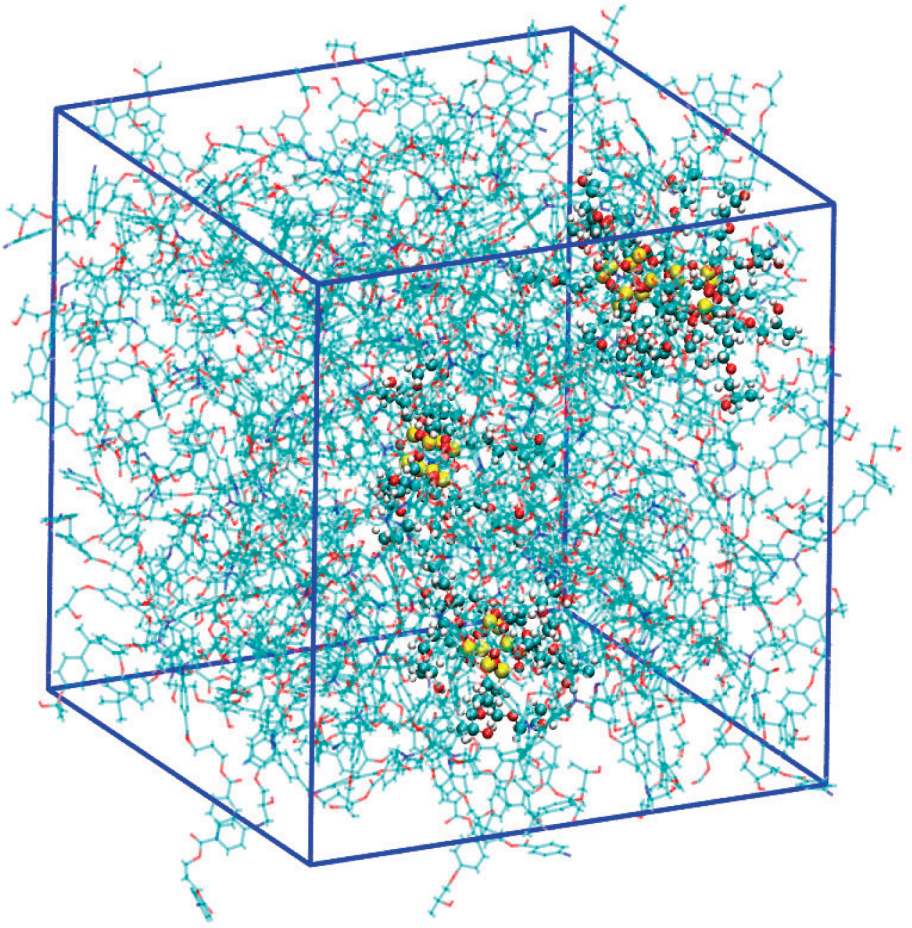

Figure 5. A built cross-linked epoxy−POSS nanocomposite structure at a density of 1.188 g/cm^3. The simulation box size is 5.31 nm. For the epoxy, carbon and nitrogen atoms are shown in blue color while oxygen atoms are shown in red color, and the hydrogen atoms have been removed for the sake of clarity. POSS particles are shown in the CPK representation.

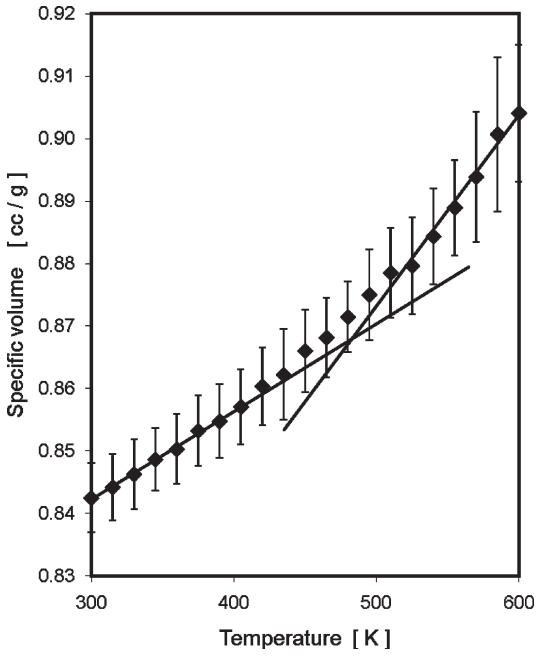

Figure 6. Volume−temperature behavior of the cross-linked epoxy structures. The linear fits to the rubbery and glassy regions are also shown.

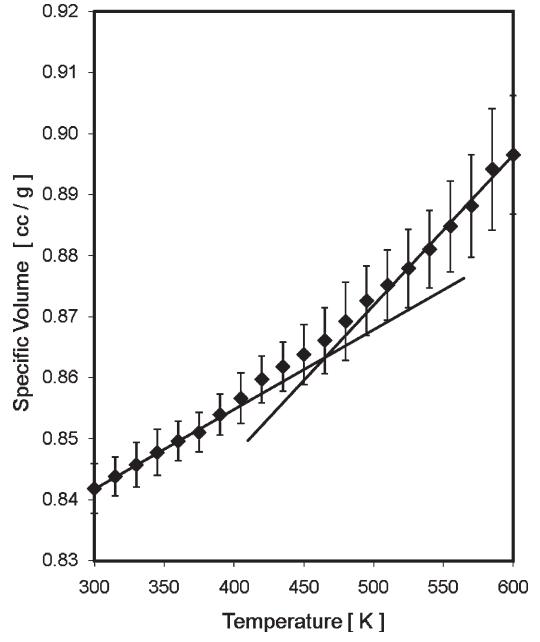

Figure 7. Volume−temperature behavior of the cross-linked epoxy−POSS structures. The linear fits to the rubbery and glassy regions are also shown.

the specific volume on the temperature both above and below the glass transition temperature. The T_g of the cross-linked epoxy−POSS system is 477 ± 5 K. The lower uncertainty of the measured values for cross-linked epoxy−POSS can be partly attributed to the larger size of these structures (14916 atoms compared with 6950 atoms for cross-linked epoxy). These values lead us to conclude that for the POSS loading studied in this work incorporation of the POSS molecules in the cross-linked epoxy structures does not change its T_g (or the change is very small and is within the statistical uncertainties of the simulations). This observation is to be compared with the experimental measurements for T_g of nanocomposites consisting of DGEBA and POSS containing eight side chains; these studies have reported that the incorporation of POSS leads to either a decrease in T_g,[46,47] a very small change (or slight lowering) in T_g,[48] or a very small increase in T_g.[41] We further note that this comparison with experiments should be considered keeping in mind that when compared to the specific chemical system studied in this work, these experimental studies have either used a different cross-linker, used a different weight percent of POSS, or used a different chemistry of POSS (e.g., different functional group on the side chains or a mixture of POSS particles that contained oligomers such as dimers of POSS). The density of the cross-linked epoxy−POSS structure as determined from simulation at 300 K is 1.188 ± 0.006 g/cm^3. Once again, we conclude that incorporation of the POSS particles (at the level of 5 wt %) in the cross-linked epoxy structure does not cause a measurable change in its density.

Table 1. Comparison of the Coefficient of Volume Thermal Expansion (CVTE) for the Cross-Linked Epoxy and Epoxy−POSS Systems As Determined from Simulation and Experiments[41]

structure	CVTE-glassy [1/K]	CVTE-rubbery [1/K]
epoxy (sim)	$(1.65 \pm 0.49) \times 10^{-4}$	$(3.43 \pm 0.78) \times 10^{-4}$
epoxy (exp)	1.86×10^{-4}	N/A
epoxy−POSS (sim, 5 wt %)	$(1.54 \pm 0.31) \times 10^{-4}$	$(2.79 \pm 0.66) \times 10^{-4}$
epoxy−POSS (exp, 2 wt %)	1.76×10^{-4}	N/A
epoxy−POSS (exp, 10 wt %)	1.88×10^{-4}	N/A

The $V-T$ data were also used to determine the coefficient of volume thermal expansion (CVTE), which is defined as

$$\alpha = \frac{1}{V_0}\left(\frac{\partial V}{\partial T}\right)_P$$

where P, V, and T are the pressure, volume, and temperature of the system, respectively, and V_0 is the volume at a specific temperature. Table 1 compares the simulated values of CVTE with those obtained from experiments for both cross-linked epoxy and the epoxy−POSS nanocomposite. The simulated values of CVTE were obtained from the slope of the $V-T$ graph over a temperature range (300−390 K for the glassy state and 510−600 K for the rubbery state) with V_0 being the volume of the system at temperature of 300 K. The experimental values used for comparison were taken as three times the coefficient of linear thermal expansion (CLTE); the CLTE values were determined in these experiments from the length change over a temperature range of 333−373 K (glassy state only) and using the length (analogous to V_0) at a temperature of 298 K.[41] For both cross-linked epoxy and the epoxy−POSS nanocomposite in the glassy state, the CVTE values predicted from simulations are lower than the corresponding experimental values. The degree of cross-linking in the simulated system is 100% whereas highly cross-linked experimental systems do not reach 100% conversion due to topological constraints; this factor could contribute to the lower CVTE in the simulated model systems as compared with the experimental systems. We also note that previous simulations of cross-linked epoxy systems have observed the simulated CVTE or CLTE values to be lower than,[18] in close agreement with,[49,50] or larger than[13] the experimental values. For both glassy and rubbery states, the mean values of CVTE for the epoxy−POSS nanocomposite obtained from simulations are lower than the mean values of CVTE for the neat cross-linked epoxy. However, the statistical uncertainties on these CVTE values as determined from the simulation data are large.

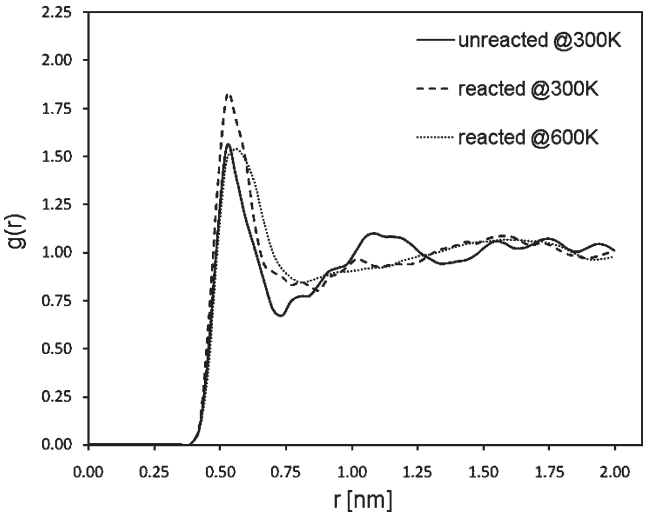

Figure 8. Radial distribution function for the DGEBA (epoxy monomer) and TMAB (cross-linker) molecule pairs. For this purpose, r denotes the distance between the central carbon atoms of the molecules.

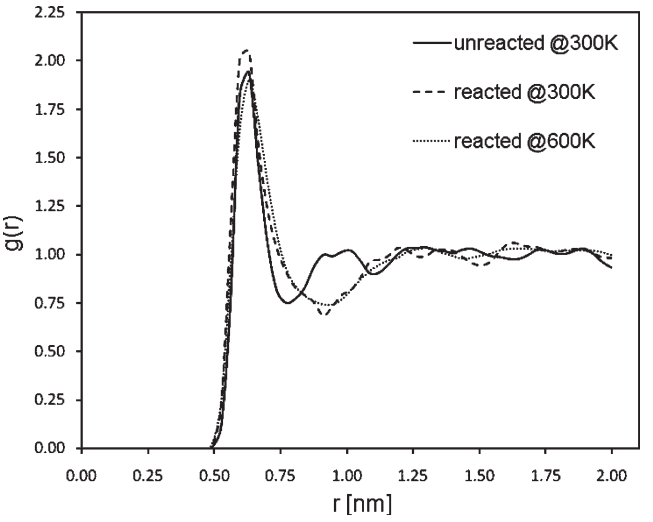

Figure 9. Radial distribution function for the DGEBA (epoxy monomer) molecule pairs. For this purpose, r denotes the distance between the central carbon atoms of the DGEBA molecules.

B. Structural Properties. In addition to the volumetric behavior, molecular simulations also yield detailed information on the molecular level structure in the system. Figure 8 shows the radial distribution function (RDF) for the epoxy monomer−cross-linker pairs in the system. For the purposes of this calculation, the distance between these molecules is taken to be the distance between the central carbon atoms of the molecules. As can be seen from the figure, even in the unreacted mixture, the RDF shows occurrence of a well-defined first peak at a distance of 0.53 nm and a weak second peak. Upon cross-linking, the height of the first peak in DGEBA−TMAB RDF shows a small increase at 300 K; however, the second peak weakens as well as broadens considerably. In both unreacted and reacted states, the RDF approaches a value of unity at longer distances, thus indicating a lack of long-range order in the system. We also note that the height of the first peak in the reacted state decreases with an increase in the temperature; we attribute this behavior to the reduction in the density of the system.

Figure 9 shows the RDF for the epoxy−epoxy pairs in the system. The RDF shows a strong first peak around 0.63 nm for both unreacted and reacted states. For the unreacted state, the RDF approaches a value of unity around a distance of 0.9 nm, whereas for the reacted state, this occurs at a longer separation distance of around 1.15 nm. We attribute this to the presence of larger amounts of cross-linker molecules near the epoxy at a distance of around 0.75 nm (see Figure 8) in the reacted state. Again, the greater height of the first peak in the reacted state at 300 K as compared to 600 K is attributed to the higher density of the system at the lower temperature.

The effect of POSS particles on the molecular structure of the system can be determined by focusing on the RDF of the POSS cage and the cross-linker molecules. Figure 10 shows the RDF for the POSS−cross-linker pairs in the epoxy−POSS nanocomposite structure. The technique described by Theodorou and Suter[51] is used to calculate the RDF for distances beyond half the box length. The RDF curve for the unreacted state shows a depletion of the cross-linker molecules within 2 nm of the center of the POSS cage. Upon reaction, owing to the bond formation between the epoxy groups on the POSS arms and the amine groups on the cross-linker molecules, the local density of the cross-linker molecules in the vicinity (at ∼0.65 nm) of the POSS cage increases. The POSS−epoxy RDF (not shown) does not

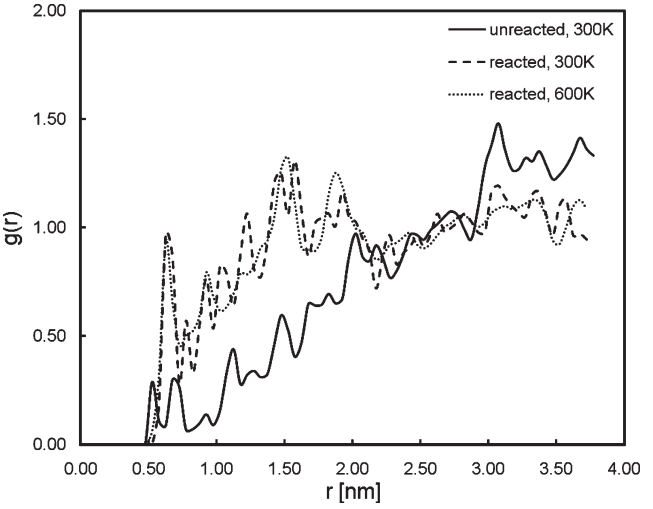

Figure 10. Radial distribution function for POSS and TMAB (cross-linker) molecule pairs. For this purpose, r denotes the distance between the geometric center of the POSS cage and the central carbon atom of the TMAB molecule.

display such a large change in the packing of the epoxy monomers around the POSS cage in the reacted and unreacted states. In both cases, the RDF shows nonzero values beyond a steric depletion layer of about 0.55 nm, eventually reaching a value close to unity at separation distances of about 1 nm. There are only four POSS particles in each of the five nanocomposite model structures that we generated. Furthermore, owing to their large mass as well as cross-linking, these do not exhibit large displacements during the simulation run. As a result, the RDF for the POSS−POSS pairs (not shown) is very noisy. This RDF indicates that the distance of closest approach of two POSS particles (note that each has eight side chains attached to them) is around 0.9 nm, and there is a significant probability of finding POSS pairs in the separation range of 1−1.5 nm.

Finally, for both the reacted and unreacted states, the orientational order in the system was characterized by calculating the orientational order parameter $P_2(r) = {}^1/_2(3\langle\cos^2\theta\rangle - 1)$, where θ is the angle between the two vectors associated with the molecules of interest (end-to-end vectors were used in this particular analysis) that are separated by a distance r. An inspection of this order

parameter for the various pairs of molecules in the system (i.e., epoxy monomers and cross-linkers) indicated lack of any noticeable orientational order in the system with respect to the end-to-end vectors.

Summary and Discussion

We have presented an efficient approach for generating atomistic model structures of cross-linked epoxy as well as a nanocomposite formed by the incorporation of POSS particles in cross-linked epoxy. Five model structures for each of these two systems were prepared using this method. The procedure did not require any iterations for the cross-linked epoxy system whereas for the system with additional architectural complexities (POSS particles that are connected with the cross-linkers via eight functionalized arms), very few iterations were required in the bond creation step.

In the stepwise cross-linking approaches in which the epoxy monomers are cross-linked in steps (as they approach within a certain reaction radius after a MD simulation run), in the late stages, the rate of the structure generation process is controlled by the diffusion of the monomers in a partially cross-linked matrix to reach the remaining reactive sites. With an increase in conversion, the fraction of remaining active sites in the system decreases, whereas the rate of diffusion slows down even further due to increased degree of cross-linking, thus causing a further slow-down of the process. We have circumvented this problem by achieving the polymerization of the entire set of monomer and cross-linker molecules in a single step. In this approach, the diffusion of the monomer and the cross-linker occurs in the initial molecular mixture, thus avoiding the need for diffusion through a partially cross-linked matrix.

We have not optimized the force field parameters to obtain exact agreement with the experimental data for the volumetric properties of the systems studied. In spite of this, we are encouraged with the level of agreement that is observed with respect to the glass transition temperature and the room temperature density. Specifically, the glass transition temperature of the cross-linked epoxy matrix determined in our simulations is about 27 K higher than the experimentally measured value. This observation is consistent with the rate of cooling in our simulations being about 11 orders of magnitude higher than that in a typical experiment. The density of the cross-linked epoxy matrix at room temperature as determined in our simulations is found to be lower than the experimental value. Again this observation is consistent with the glass transition temperature in simulations being higher than the experimental one due to the very high cooling rates. Such a glass formed at a higher temperature is expected to have a lower density.

Our simulation results indicate that incorporation of functionalized POSS particles at 5 wt % in the cross-linked epoxy matrix does not lead to a measurable change in the glass transition temperature or the room temperature density of this nanocomposite as compared with the neat cross-linked epoxy. The POSS containing epoxy resin shows a tendency for lower values of CVTE in both the rubbery and the glassy states than the neat cross-linked epoxy. Such lower values of CVTE could potentially help reduce the thermal stresses in the resin. The relative magnitude of the uncertainties (as a fraction of the mean) in the CVTE values is larger compared with the uncertainties in the T_g values. Simulations on much larger systems will be required to reduce these uncertainties; this will be one of the goals of the future work.

The method presented in this work for building models of cross-linked polymer matrices and their nanocomposites is general and can be applied for the generation of atomistic model structures of other polymer nanocomposite systems. In our current implementation, we explicitly prevented formation of intramolecular loops in the epoxy−POSS nanocomposite. This restriction can be relaxed in future work to quantify the effects of such loop formation on the mechanical properties of the system. Furthermore, by construction, our cross-linked systems exhibit 100% conversion. In future work, the method can be readily modified to control the degree of cross-linking to a specified level and determine the effect of network defects such as dangling loops on the properties of the system.

Acknowledgment. Financial support received from National Aeronautics and Space Administration (NASA, Contract NNX07AD44A) for this work is gratefully acknowledged. The authors thank Sindee Simon and Qingxiu Li for the discussions of the experimental data.

Supporting Information Available: Values of force field parameters that are used to supplement the gaff[26,27] parameters as well as the adjusted values of partial charges. This material is available free of charge via the Internet at http://pubs.acs.org.

References and Notes

(1) Pham, H. Q.; Marks, M. J. In *Encyclopedia of Polymer Science and Technology*, 3rd ed.; Kroschwitz, J. I., Ed.; Wiley: Hoboken, NJ, **2004**; Vol. *9*, pp 678−804.
(2) Paul, D. R.; Robeson, L. M. *Polymer* **2008**, *49*, 3187–3204.
(3) Winey, K. I.; Vaia, R. A. *MRS Bull.* **2007**, *32*, 314–319.
(4) Ganesan, V. *J. Polym. Sci., Part B: Polym. Phys.* **2008**, *46*, 2666–2671.
(5) Theodorou, D. N.; Suter, U. W. *Macromolecules* **1985**, *18*, 1467–1478.
(6) Boyd, R. H. *Macromolecules* **1989**, *22*, 2477–2481.
(7) Hutnik, M.; Gentile, F. T.; Ludovice, P. J.; Suter, U. W.; Argon, A. S. *Macromolecules* **1991**, *24*, 5962–5969.
(8) Rapold, R. F.; Suter, U. W.; Theodorou, D. N. *Macromol. Theory Simul.* **1994**, *3*, 19–43.
(9) Rigby, D.; Roe, R. J. *J. Chem. Phys.* **1987**, *87*, 7285–7292.
(10) Khare, R.; Paulaitis, M. E.; Lustig, S. R. *Macromolecules* **1993**, *26*, 7203–7209.
(11) Kotelyanskii, M.; Wagner, N. J.; Paulaitis, M. E. *Macromolecules* **1996**, *29*, 8497–8506.
(12) Queyroy, S.; Neyertz, S.; Brown, D.; Muller-Plathe, F. *Macromolecules* **2004**, *37*, 7338–7350.
(13) Komarov, P. V.; Chiu, Y. T.; Chen, S. M.; Khalatur, P. G.; Reineker, P. *Macromolecules* **2007**, *40*, 8104–8113.
(14) Doherty, D. C.; Holmes, B. N.; Leung, P.; Ross, R. B. *Comput. Theor. Polym. Sci.* **1998**, *8*, 169–178.
(15) Heine, D. R.; Grest, G. S.; Lorenz, C. D.; Tsige, M.; Stevens, M. J. *Macromolecules* **2004**, *37*, 3857–3864.
(16) Yarovsky, I.; Evans, E. *Polymer* **2002**, *43*, 963–969.
(17) Wu, C. F.; Xu, W. J. *Polymer* **2006**, *47*, 6004–6009.
(18) Varshney, V.; Patnaik, S. S.; Roy, A. K.; Farmer, B. L. *Macromolecules* **2008**, *41*, 6837–6842.
(19) Case, D. A.; Cheatham, T. E.; Darden, T.; Gohlke, H.; Luo, R.; Merz, K. M.; Onufriev, A.; Simmerling, C.; Wang, B.; Woods, R. J. *J. Comput. Chem.* **2005**, *26*, 1668–1688.
(20) Wang, J. M.; Wang, W.; Kollman, P. A. *Abstr. Pap. Am. Chem. Soc.* **2001**, *222*, U403–U403.
(21) Jakalian, A.; Bush, B. L.; Jack, D. B.; Bayly, C. I. *J. Comput. Chem.* **2000**, *21*, 132–146.
(22) Jakalian, A.; Jack, D. B.; Bayly, C. I. *J. Comput. Chem.* **2002**, *23*, 1623–1641.
(23) Stubbs, J. M.; Potoff, J. J.; Siepmann, J. I. *J. Phys. Chem. B* **2004**, *108*, 17596–17605.
(24) Wick, C. D.; Stubbs, J. M.; Rai, N.; Siepmann, J. I. *J. Phys. Chem. B* **2005**, *109*, 18974–18982.
(25) Sun, H.; Rigby, D. *Spectrochim. Acta, Part A* **1997**, *53*, 1301–1323.
(26) Wang, J. M.; Wolf, R. M.; Caldwell, J. W.; Kollman, P. A.; Case, D. A. *J. Comput. Chem.* **2004**, *25*, 1157–1174.
(27) Wang, J. M.; Wang, W.; Kollman, P. A.; Case, D. A. *J. Mol. Graphics* **2006**, *25*, 247–260.
(28) Smith, J. S.; Borodin, O.; Smith, G. D. *J. Phys. Chem. B* **2004**, *108*, 20340–20350.

(29) Habenschuss, A.; Tsige, M.; Curro, J. G.; Grest, G. S.; Nath, S. K. *Macromolecules* **2007**, *40*, 7036–7043.
(30) Berendsen, H. J. C.; Vanderspoel, D.; Vandrunen, R. *Comput. Phys. Commun.* **1995**, *91*, 43–56.
(31) Lindahl, E.; Hess, B.; van der Spoel, D. *J. Mol. Model.* **2001**, *7*, 306–317.
(32) Van der Spoel, D.; Lindahl, E.; Hess, B.; Groenhof, G.; Mark, A. E.; Berendsen, H. J. C. *J. Comput. Chem.* **2005**, *26*, 1701–1718.
(33) Darden, T.; York, D.; Pedersen, L. *J. Chem. Phys.* **1993**, *98*, 10089–10092.
(34) Hoover, W. G. *Phys. Rev. A* **1985**, *31*, 1695–1697.
(35) Nose, S. *Mol. Phys.* **1984**, *52*, 255–268.
(36) Nose, S.; Klein, M. L. *Mol. Phys.* **1983**, *50*, 1055–1076.
(37) Parrinello, M.; Rahman, A. *J. Appl. Phys.* **1981**, *52*, 7182–7190.
(38) Kirkpatrick, S.; Gelatt, C. D.; Vecchi, M. P. *Science* **1983**, *220*, 671–680.
(39) Press, W. H.; Flannery, B. P.; Teukolsky, S. A.; Vetterling, W. T. *Numerical Recipes in FORTRAN 77: The Art of Scientific Computing*; Cambridge University Press: New York, **1992**.
(40) Wang, X. R.; Gillham, J. K. *J. Coat. Technol.* **1992**, *64*, 37–45.
(41) Li, Q.; Hutcheson, S. A.; McKenna, G. B.; Simon, S. L. *J. Polym. Sci., Part B: Polym. Phys.* **2008**, *46*, 2719–2732.
(42) Venditti, R. A.; Gillham, J. K.; Jean, Y. C.; Lou, Y. *J. Appl. Polym. Sci.* **1995**, *56*, 1207–1220.
(43) Badrinarayanan, P.; Zheng, W.; Li, Q. X.; Simon, S. L. *J. Non-Cryst. Solids* **2007**, *353*, 2603–2612.
(44) Pang, K. P.; Gillham, J. K. *J. Appl. Polym. Sci.* **1989**, *37*, 1969–1991.
(45) Wang, X. R.; Foltz, V. J. *Polymer* **2006**, *47*, 5090–5096.
(46) Pellice, S. A.; Fasce, D. P.; Williams, R. J. J. *J. Polym. Sci., Part B: Polym. Phys.* **2003**, *41*, 1451–1461.
(47) Brus, J.; Urbanova, M.; Strachota, A. *Macromolecules* **2008**, *41*, 372–386.
(48) Liu, Y. H.; Zheng, S. X.; Nie, K. M. *Polymer* **2005**, *46*, 12016–12025.
(49) Fan, H. B.; Yuen, M. M. F. *Polymer* **2007**, *48*, 2174–2178.
(50) Wu, C. F.; Xu, W. J. *Polymer* **2007**, *48*, 5802–5812.
(51) Theodorou, D. N.; Suter, U. W. *J. Chem. Phys.* **1985**, *82*, 955–966.